PLOS ONE

RESEARCH ARTICLE

An inversion model for estimating the negative air ion concentration using MODIS images of the Daxing'anling region

Cui Yue, Zhao Yuxin, Zhang Nan, Zhang Dongyou◉*, Yang Jiangning

Heilongjiang Province Key Laboratory of Geographical Environment Monitoring and Spatial Information Service in Cold Regions, Harbin Normal University, Harbin, China

* zhangdy@hrbnu.edu.cn

Abstract

The negative air ion (NAI) concentration is an essential indicator of air quality and atmospheric pollution. The NAI concentration can be used to monitor air quality on a regional scale and is commonly determined using field measurements. However, obtaining these measurements is time-consuming. In this paper, the relationship between remotely sensed surface parameters (such as land surface temperature, normalized difference vegetation index (NDVI), and leaf area index) obtained from MODIS data products and the measured NAI concentration using a stepwise regression method was analyzed to estimate the spatial distribution of the NAI concentration and verify the precision. The results indicated that the NAI concentration had a negative correlation with temperature, leaf area index (LAI), and gross primary production while it exhibited a positive correlation with the NDVI. The relationship between land surface temperature and the NAI concentration in the Daxing'anling region is expressed by the regression equation of $y = -35.51x_1 + 11206.813$ ($R^2 = 0.6123$). Additionally, the NAI concentration in northwest regions with high forest coverage was higher than that in southeast regions with low forest coverage, suggesting that forests influence the air quality and reduce the impact of environmental pollution. The proposed inversion model is suitable for evaluating the air quality in Daxing'anling and provides a reference for air quality evaluation in other areas. In the future, we will expand the quantity and distribution range of sampling points, conduct continuous observations of NAI concentrations and environmental parameters in the research areas with different land-use types, and further improve the accuracy of inversion results to analyze the spatiotemporal dynamic changes in NAI concentration and explore the possibility of expanding the application areas of NAI monitoring.

Introduction

Negative air ions (NAI) are negatively charged atoms or molecules in the atmosphere. NAI mainly consist of negative oxygen ions because the "capture" ability of oxygen is stronger than that of other air molecules, and oxygen has easy access to the free electrons of the NAI [1].

NAI in nature are generally produced by ionization, the Lenard effect, the point discharge of plant tips, the photoelectric effect, and other atmospheric discharge phenomena such as lighting and thunderstorms; the effective method of artificially generating NAI is corona discharge [2].

NAI can improve the physiology of people and maintain their health at certain levels of concentration [3]. At NAI concentrations of more than 1,000 ind/cm^3, beneficial health effects have been observed; and at NAI concentration of 8,000 ind/cm^3, diseases have been cured [4–7]. In contrast, at NAI concentrations of less than 40~50 ind/cm^3, people may experience headaches and insomnia. High NAI concentrations can relieve depression, improve basic information processing capacity, as well as prevent and cure cognition impairment [8–10]. Besides, negative oxygen ions can improve people's sleep quality and blood circulation, enhance cardiopulmonary functions, aerobic metabolism, and recovery after movements, as well as cure pneumoconiosis by integrating with low load aerobic Yoga [11–15]. An NAI generator can eliminate particulate matters in the atmosphere while filtering and inactivating aerosolized viruses [16–19]. Therefore, an investigation of the NAI concentration is of great significance for human physical and mental health and the improvement of air quality.

NAI research has become an essential topic in recent years. International research on air anions has primarily focused on the effects of air anions on biological organisms, clinical medical applications, spatiotemporal distribution and air quality evaluation [20–23]. The spatial and temporal variations of NAI and their influencing factors have attracted much attention [24]. Studies have revealed that NAI concentrations depended mainly on location, vegetation characteristics, climate, and meteorological conditions. For example, NAI concentrations were demonstrated to be higher in summer than in winter [25, 26]. With the premise of controlling other variables, the NAI concentration could be improved by increasing the number of plants and exerting pulsed electric fields (PEF) on vegetation [27–29]. From the perspective of area research, the NAI concentration of falls and forests is generally higher than that of greenbelts and bare lands [30, 31]. Since most research on NAI concentrations in China was conducted in southern and coastal areas, the results may not apply to northern China, and the traditional anion concentration study is generally in a limited area. During the past few years, research activity on this topic has been increased overseas while these studies have emphasized small areas and conducted qualitative analyses; there is little research on the temporal and spatial distribution of NAI and the retrieval of NAI with inversion models [25]. During the practical application processes, it is difficult for researchers to grasp the spatial distribution of NAI concentration; obstructing some works such as air quality monitoring, health care, and urban planning. The innovation of our paper is to use remote sensing data to study the anion concentration in a large area.

In this study, an inversion model of the NAI concentration was developed using remotely sensed data of the Daxing'anling region. Forty-four sample points were adopted in different land cover types. Besides, field measurements of the NAI concentration were conducted in the summer of 2016. Afterward, the key environmental factors affecting the NAI concentration were determined, and a relationship between these factors and the NAI concentration was developed. Finally, an evaluation of the above research results was performed, and the utilization potentiality and scientific values of NAI concentration inversion in future researches were discussed.

Methods and materials

Study area

The Daxing'anling region (50°08' -53°34' N, 121°11'-127°00' E) is located in the north of Heilongjiang province and northeast of Inner Mongolia; the area is the largest and northernmost
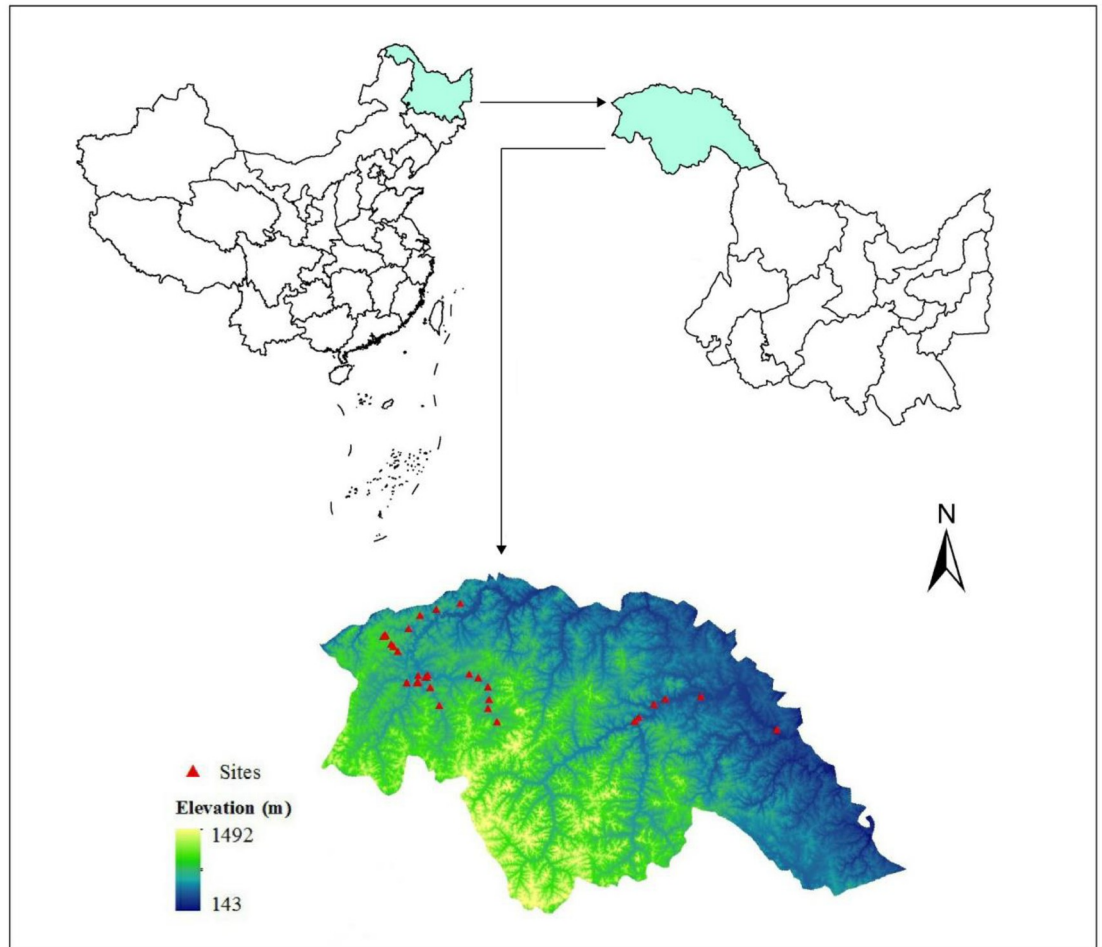
Fig 1. Location of the study area.

forest region in China, significant to forestry [32]. The Daxing'anling region covers 64,800 km², high-elevation areas occur in the west; low-elevation areas occur in the east with gentle terrain slopes (Fig 1). The Daxing'anling region has dense virgin forests, and the dominant trees are Xingan larch, camphor pine, red spruce, white birch, Mongolian oak, and aspen.

Data source and processing

Field sampling of NAI concentration. Field sampling was conducted in late July of 2016 due to active vegetation growth and peak photosynthesis in the summer. The samples were obtained in five land use/landcover types: forest land, grassland, cultivated land, buildings, and water (S1 Table). The predominant types of land cover were grassland and woodland. With the purpose of controlling sampling time, reducing plant physiological activities and surface temperature changes caused by seasonal factors, and improving data acquisition efficiency, sampling points in this research were laid along the roads with an equal interval as far as possible and a distance of at least 1 km from the main roads to avoid the influence of passing vehicles on the NAI concentration [33].

GPS measurements of latitude and longitude were collected at each site; the negative and positive ion concentrations at 150 cm above the ground were obtained using an air ion counter

(COM-3200-PRO) on a tripod. Operators should keep a distance of 2~3m from the equipment while measuring to record the reading after it was stabilized, with an error of ≤±5%.

All measurements were obtained under clear and calm weather conditions and at least 50 m inside the forest canopy to minimize the influence of weather, fog, and environmental pollution.

MODIS images. In this study, MODIS data were used to develop the inversion model of the NAI concentration. The data were downloaded from the United States Geological Service (USGS) website (http://glovis.usgs.gov). Four data products (MOD11A2, MOD13A3, MOD15A2, and MOD17A2) for July 2016 were employed to extract LST, NDVI, LAI, and GPP, respectively.

Study method

Data acquired through remote sensing technology is of an outstanding space-time coverage and continuity, making it suitable for monitoring vegetation indexes and climate conditions [34, 35]. Vegetational covers and climate changes can be broadly, simply, and efficiently measured through vegetation index; this may have certain correlations with the formation of NAI in nature while no relevant literature has been found up to now. In this paper, the relationships between remote sensing surface parameters (land surface temperature, normalized difference vegetation index (NDVI), leaf area index, etc.) were firstly analyzed by MODIS data products; then, the spatial distribution and accuracy of the negative ion concentration were estimated by correlation analysis and stepwise regression analysis.

Environmental parameters. The MODIS reprojection tool (MRT) was used to convert the HDF format to the TIF format and reproject and resample the data. Besides, ArcGIS 10.1 was adopted to crop the MODIS image to the Daxing'anling region and obtain a TIF format image. Similarly, TIF raster images of the land surface temperature (LST), normalized difference vegetation index (NDVI = (NIR - R)/(NIR + R), NIR: Near-infrared reflectance, R: Red band reflectance), leaf area index (LAI = total leaf area/land area), and gross primary production (GPP: an indicator of vegetation growth) were obtained. Particularly, the clipped MODIS images were filtered with a 3×3 mean filter to smooth the image before the ground scene information was extracted from the data owing to the difference in scale between the MODIS image resolutions and the locations of sampling points that were not located in homogeneous areas. The pixel value within the whole window was balanced through this method, contributing to more accurately reflecting the environmental characteristics of the sampling points and avoiding accidental errors. The mapping results are illustrated in Fig 2.

The vector file with the sample locations and the LST, NDVI, LAI, and GPP raster files were in the same projection to ensure that the data for the correct location were extracted from the raster files. The numerical results are presented in Table 1.

The LST was retrieved using the equation $NEW\_DN = OLD\_DN * 0.02$, where OLD_DN denotes the gray value of a pixel of MOD11A2, and NEW_DN represents brightness temperature in Kelvin.

Correlation and regression analysis. Correlation coefficient r between the parameter values calculated by the SPSS software and the measured NAI concentrations is expressed in Formula 1.

Regression analysis refers to a statistical analysis method used to determine the quantitative relationship between two or more variables. In this study, the regression analysis of the relationship between the NAI concentration and the environmental parameters was conducted using SPSS, and the linear regression models was acquired through a backward regression method. Through backward regression, all environmental parameters were first selected into
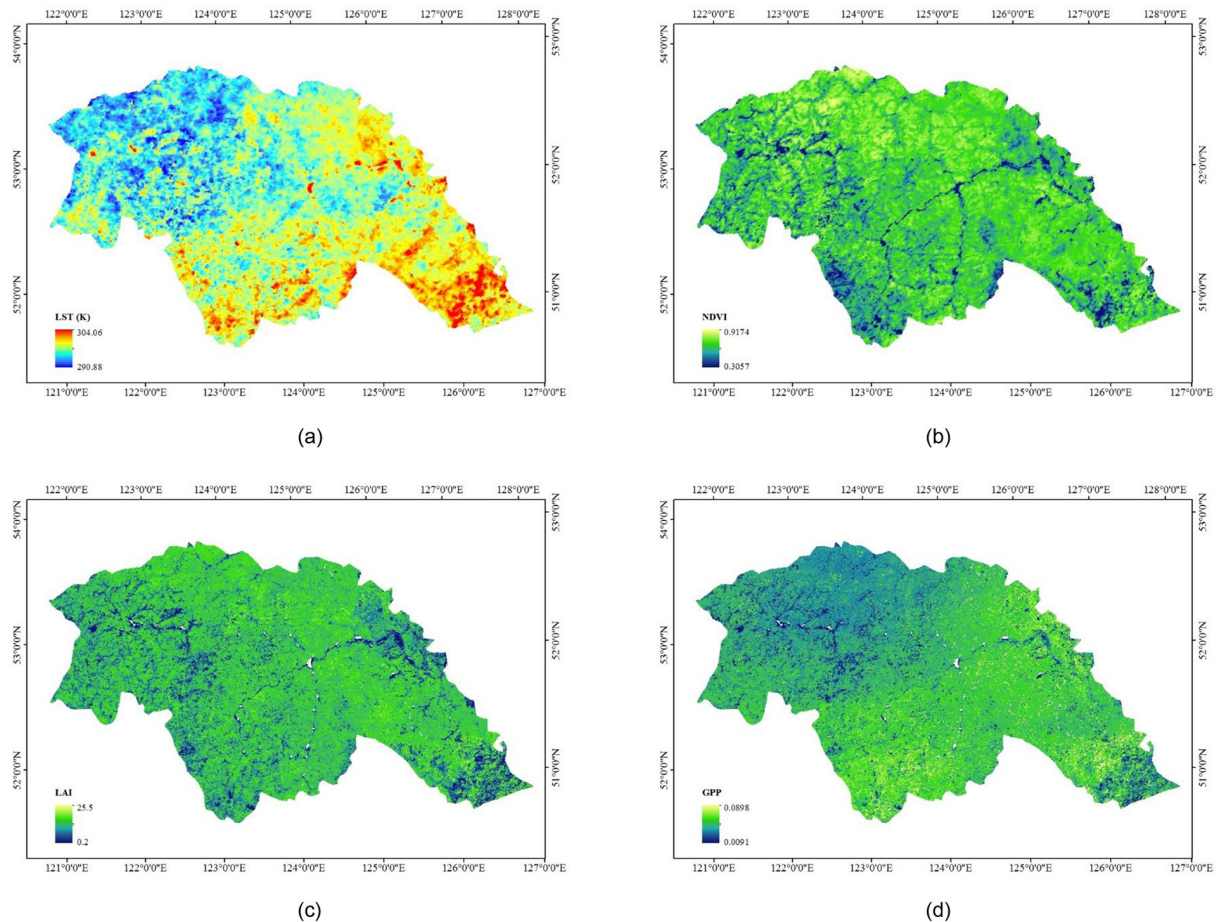
Fig 2. MODIS-based LST (a), NDVI (b), LAI (c), and GPP (d) of the Daxing'anling region.

an inversion regression equation; then, full consideration was given to the combination effect of independent variables; next, those variables with an indistinctive influence on the regression equation were eliminated in order; finally, an inversion model was established and verified by the RMSE (Eqs 2 and 3).

$$r = \frac{\sum_{i=1}^{n}(x_i - \bar{x})(y_i - \bar{y})}{\sqrt{\sum_{i=1}^{n}(x_i - \bar{x})^2 \sum_{i=1}^{n}(y_i - \bar{y})^2}} \tag{1}$$

$$e_i = x_i - x_i' (i = 1, 2, \cdots, n) \tag{2}$$

$$RMSE = \sqrt{\frac{1}{n}\sum_{i=1}^{n}e_i^2} \tag{3}$$

where n denotes the number of sampling points; x_i and y_i are measured value of NAI concentration and environmental parameter at the ith sampling point (i.e. extracted value of LST, NDVI, LAI, and GPP), respectively; $\bar{x}$ and $\bar{y}$ refer to the mean values of NAI concentration

Table 1. Values of the four parameters (GPP, LAI, LST, and NDVI) at the sampling points.

Sample point	GPP	LAI	LST	NDVI	Sample point	GPP	LAI	LST	NDVI
1	0.11	3.44	291.96	0.87	23	0.11	4.76	295.70	0.84
2	0.12	4.03	292.40	0.86	24	0.12	4.16	295.73	0.80
3	0.10	2.51	293.05	0.79	25	0.12	4.16	295.73	0.80
4	0.11	3.00	293.72	0.84	26	0.11	4.80	295.92	0.87
5	0.11	4.30	293.87	0.84	27	0.11	3.01	295.97	0.80
6	0.08	1.12	293.91	0.81	28	0.12	4.41	296.09	0.85
7	0.11	3.56	294.16	0.83	29	0.12	4.41	296.09	0.85
8	0.11	3.67	294.19	0.83	30	0.10	3.28	296.63	0.80
9	0.11	3.53	294.20	0.82	31	0.11	3.69	296.63	0.77
10	0.11	3.53	294.20	0.82	32	0.11	3.69	296.63	0.77
11	0.10	2.97	294.31	0.82	33	0.11	3.69	296.63	0.77
12	0.13	5.16	294.39	0.88	34	0.11	3.69	296.63	0.77
13	0.11	3.96	294.74	0.80	35	0.11	3.69	296.63	0.77
14	0.11	3.79	294.91	0.83	36	0.11	3.69	296.63	0.77
15	0.11	3.79	294.91	0.83	37	0.11	3.69	296.63	0.77
16	0.12	4.09	295.12	0.82	38	0.09	2.13	297.42	0.69
17	0.13	4.69	295.16	0.86	39	0.09	2.13	297.42	0.69
18	0.13	4.69	295.16	0.86	40	0.09	2.13	297.42	0.69
19	0.12	4.04	295.32	0.85	41	0.10	2.86	298.47	0.71
20	0.11	3.26	295.32	0.76	42	0.10	2.86	298.47	0.71
21	0.11	3.26	295.32	0.76	43	1.86	14.49	298.53	0.48
22	0.11	4.33	295.58	0.84	44	1.86	14.49	298.53	0.48

and environmental parameter, respectively; x'_i and e_i represents the simulation value at the ith sampling point and the difference value between this simulation value and the measured value, respectively. The higher the absolute value of correlation coefficient r, the higher the correlation between NAI concentration and the above environmental parameter; when r is positive, the NAI concentration increases as the above environmental parameter increases, and vice versa. Besides, the lower the RMSE, the smaller the difference between measured and simulated values, and the higher the precision of the inversion model.

Results

Comparison of the inversion model

The relevant analysis shows that NAI is significantly negatively related with LST, GPP and LAI respectively (r = -0.782, -0.459, -0.461, P<0.01), and NAI has a significantly positive correlation with NDVI (r = 0.611, P<0.01). There was a significant relationship between the selected remotely sensed land surface parameters and the NAI concentration measured at the sampling site.

The results of backward regression are provided in Table 2. The models for LST and LAI had the form of y = -32.132x$_1$-6.343x$_2$ + 10232.557; the regression model for LST had the form of y = -35.515x$_1$ + 11206.813.

The results of the regression analysis illustrate that there is a significant correlation between LST and NAI (Fig 3), while NAI has a significant linear relationship with GPP, LAI and NDVI (S1 Fig). It is concluded that it is feasible to use MODIS images and environmental parameters (LST) to estimate the NAI concentration with an inversion model. The relationship between

Table 2. Regression results of the relationship between negative air ion concentration and environmental parameters.

	Model	Unstandardized Coefficients (B)	Standard error of B	Significance level of T (Sig)	95% lower confidence interval of B	95% upper confidence interval of B	Standardized Coefficients (Beta)
1	LST	-32.132	4.445	0	-41.109	-23.154	-0.708
	LAI	-6.343	2.872	0.033	-12.143	-0.543	-0.216
	Constant	10232.557					
2	LST	-35.515	4.361	0	-44.316	-26.714	-0.782
	Constant	11206.813					

LST and the NAI concentration in the Daxing'anling region is expressed by the regression equation of $y = -35.515x_1 + 11206.813$ ($R^2 = 0.6123$).

Results of the NAI model

The NAI concentrations in the Daxing'anling area in 2013 were obtained, and the LST-NAI regression equations were analyzed. Besides, the measured values and values of the regression equation of 17 points obtained from the same measurement method were compared by performed random sampling. The RMSE is 2.88 ind/cm^3, suggesting that this method is suitable for the estimation of the NAI concentration [36, 37].

The map of the NAI concentration in the Daxing'anling region based on the regression model is illustrated in Fig 4. The NAI concentration in the Daxing'anling region is within
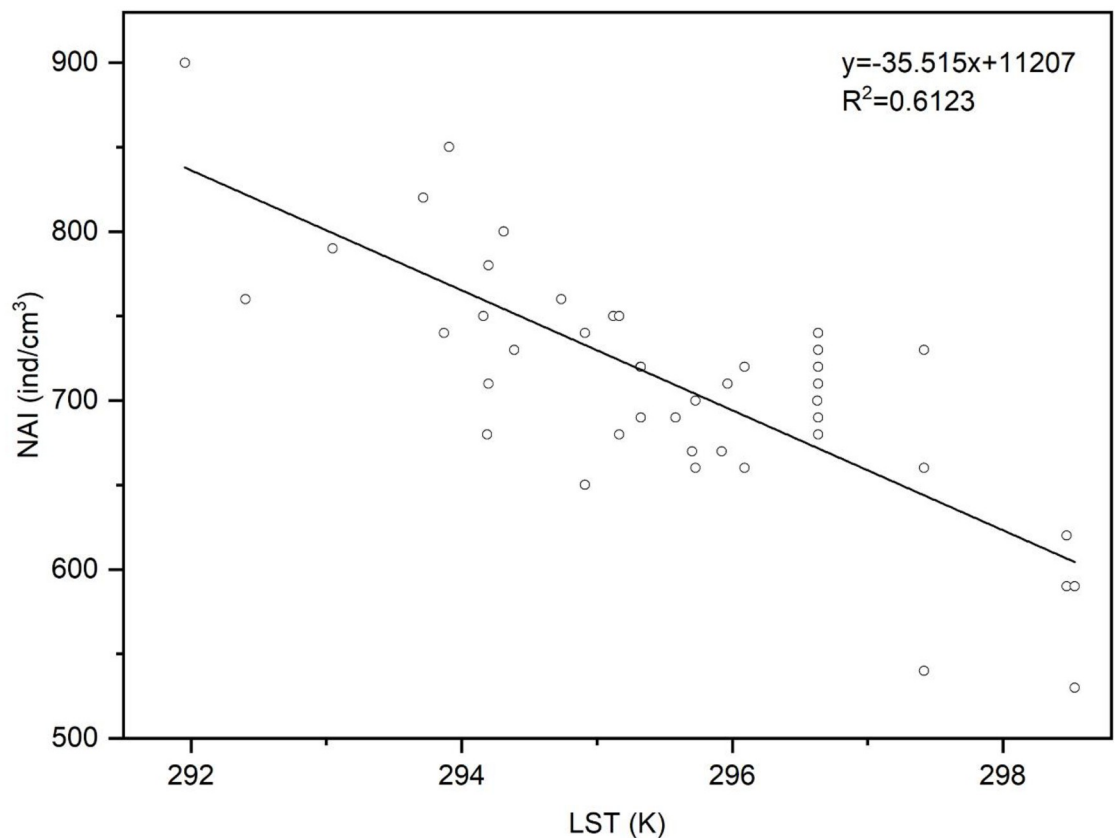

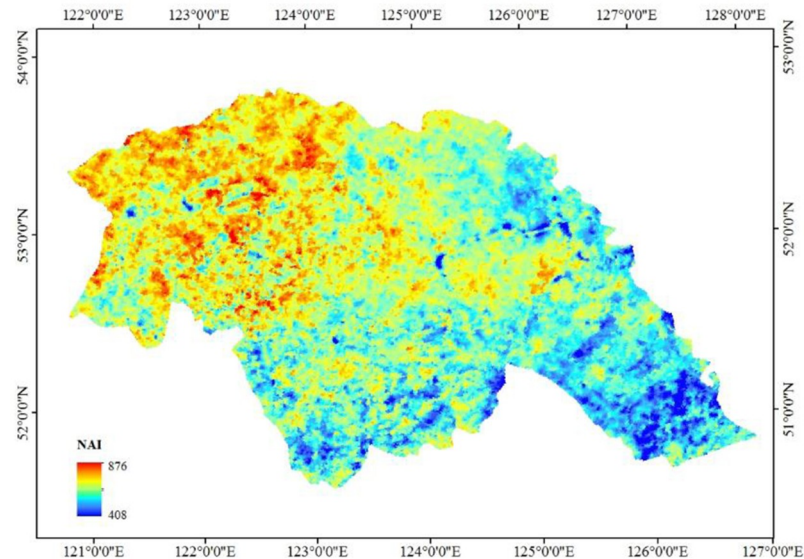Fig 3. Linear regression of LST and NAI.

Fig 4. Negative air ion concentration in the Daxing'anling region.

https://doi.org/10.1371/journal.pone.0242554.g004

$408\sim876$ ind/cm^3, exhibiting an obvious spatial difference. Non-forestlands are widely distributed in the southeast part of this region while there are a relatively higher forest coverage rate and fewer human activities in the northwest part; this may be a crucial element leading to the fact that the NAI concentration in the southeast is lower than that in the northwest.

Discussion

NAI is a valuable resource provided by forests. The concentration of NAI is an important indicator for evaluating the air quality in a region. Negative oxygen ions are also called "air vitamins" and have a positive impact on human health and the ecological environment [38–42]. Researchers have discovered that NAI has a bacteriostatic and sterilizing effect on microorganisms, leading to air purification and improvements in the ecological environment. Besides, the concentration of NAI can be used as an index to monitor urban pollution, and increasing the concentration of NAI can improve air quality and reduce air pollutants and bacterial dust. In recent years, there has been an increasing number of research on NAI monitoring and distribution characteristics, as well as the effect of NAI on the ecological environment. However, most of them are limited to small-scale measurements, focus on the analyses of differences in NAI concentrations of different land-use types and their influence factors, and are deficient in the reports of adopting the 3S technology to invert NAI concentration. With the Daxing'anling region as an example, the vegetation index and LST data extracted from local MODIS products and their correlations with NAI concentration are calculated in this research; meanwhile, the research scope of factors influencing NAI concentration is enlarged, providing beneficial references for an in-depth understanding of generating and consuming mechanisms of NAI. Establishing an inversion model based on environmental factors is a feasible method to grasp the spatial and temporal distribution of NAI and is of great utilization potential.

It is indicated in previous works that it is difficult to make a unified conclusion on the correlation between NAI and meteorological factors because of the complexity of the environment in the research area and non-standardization of monitoring equipment [43]. Most

studies have demonstrated that NAI concentrations were positively correlated with temperature [26, 44, 45] while some studies revealed a negative correlation between the NAI concentration and temperature [46, 47]. It was discovered in this research that there was a prominent negative correlation mainly between NAI concentration and LST in the Daxing'anling region; this might be because the photosynthesis in growing seasons was hindered by the ultra-high environmental temperature, resulting in influencing the rate of photoelectric effect of green plants when generating NAI [48]. NAI had a positive correlation with NDVI, suggesting that the NAI concentration level could also be affected by the growth vigor of plants [49]. The regression equation describing the relationship between NAI and LST took the form of y = -35.515x_1 + 11206.813.

The NAI concentration in the Daxing'anling region is within 408~876 ind/cm^3, presenting a distribution characteristic that the NAI concentration in the northwest is higher than that in the southeast; this conforms to the local forest distribution. The analysis indicates several reasons for the high NAI concentration in forest land: 1) the soil in forests contains large amounts of radioactive materials that promote the exchange of air in the soil, generate negative oxygen ions, and increase the concentration of NAI; 2) the photosynthesis and transpiration of plants lead to the production of NAI, and the discharge from the leaves of vegetation causes air to ionize and produces negative oxygen ions, resulting in an increase in the concentration of NAI; 3) forest land absorbs large amounts of dust, contributing to reducing the loss of negative ions by the dust and maintaining a constant concentration of NAI.

In this study, only four environmental factors (LST, GPP, LAI, and NDVI) were considered. The field monitoring data were relatively sparse, which may have affected the accuracy of the research results.

Conclusion

NAI concentrations were measured in the Daxing'anling region in late July of 2016, and MODIS images were obtained during the same period. The relationships between the remotely sensed land surface parameters (LST, NDVI, LAI, and GPP) and the measurements of the NAI concentration were determined using a stepwise regression method to estimate the NAI concentration in the Daxing'anling region. Finally, the spatial distribution of local NAI concentration was inverted. Introducing remote sensing land surface parameters into researches on NAI contributes to more accurately grasping the leading factors influencing NAI concentrations in different regions. Meanwhile, NAI concentration inversion has exhibited a preferable application prospect in several fields, including but not limited to 1) providing references for site selection of forest salutarium improve health care effect of NAI [50]; 2) exploring the changes in NAI distribution during the urbanization process, such as evaluating the influence of urban heat island and water pollution on NAI [51, 52]; 3) scientifically implementing urban planning to promote ecological benefits and human well-being [33]. Besides, the problem of a wide-range grasp of NAI concentration was initially solved by this study. However, this method also exhibits certain limitations due to inconvenient road traffic in the Daxing'anling area, deficient sampling points of NAI, and the comparison of the relationships between only 4 categories of remote sensing surface parameters and NAI concentration. In the future, we will expand sampling density and scope, conduct continuous observations of NAI concentrations and environmental parameters under different land-use types in the research area, improve the inversion model, and enhance inversion accuracy.

Supporting information

S1 Table. The location of the sampling site and the attribute information of the ground objects of the sampling site.
(DOCX)

S1 Fig. Linear trends of GPP, LAI, NDVI and NAI of sampling site.
(DOCX)

Author Contributions

Conceptualization: Zhang Dongyou.

Data curation: Cui Yue, Zhang Nan, Yang Jiangning.

Formal analysis: Cui Yue, Zhao Yuxin, Zhang Nan.

Funding acquisition: Zhang Dongyou.

Investigation: Zhao Yuxin, Yang Jiangning.

Methodology: Zhang Dongyou, Yang Jiangning.

Project administration: Zhang Dongyou.

Resources: Cui Yue, Yang Jiangning.

Supervision: Zhang Dongyou.

Validation: Cui Yue.

Visualization: Zhao Yuxin, Zhang Nan.

Writing – original draft: Cui Yue, Yang Jiangning.

Writing – review & editing: Zhao Yuxin, Zhang Nan.

References

1. Zhang XK, Cao JX, Zhang SY. Distribution characteristics of air anions in Beidaihe in different ecological environments. Journal of Geoscience and Environment Protection. 2018; 6(5):133–150.

2. Jiang S, Ma A, Ramachandran S. Negative air ions and their effects on human health and air quality improvement. Int J Mol Sci. 2018; 19(10):2966. https://doi.org/10.3390/ijms19102966 PMID: 30274196

3. Li AB. The research progress of air ion experiments and clinical study. Chinese Journal of Physical Therapy. 2001; 24(2):53–56.

4. Shal'nova GA. Air ionization and its effects on the immune system of man and animals. Radiats Biol Radioecol. 1994; 34(3):391–397. PMID: 8069374

5. Malcolm CP, Cowen PJ, Harmer CJ. High-density negative ion treatment in creases positive affective memory. Psychol Med. 2009; 39(11):1930–1932. https://doi.org/10.1017/S0033291709990444 PMID: 19619385

6. Kosenko EA, Kaminsky YG, Stavrovskaya IG, Sirota TV, Kondrashova MN. The stimulatory effect of negative air-ions and hydrogen peroxide on the activity of superoxide dismutase. FEBS Lett. 1997; 410 (2/3):309–312. https://doi.org/10.1016/s0014-5793(97)00651-0 PMID: 9237652

7. Peng ZH. Chinese urban forest. Beijing: China Forestry Publishing Ho.; 2003.

8. Bowers B, Flory R, Ametepe J, Staley L, Patrick A, Carrington H. Controlled trial evaluation of exposure duration to negative air ions for the treatment of seasonal affective disorder. Psychiatry Res. 2018; 259:7–14. https://doi.org/10.1016/j.psychres.2017.08.040 PMID: 29024857

9. Della Vecchia A, Mucci F, Pozza A, Marazziti D. Negative air ions in neuropsychiatric disorders. Curr Med Chem. 2020 Jun 29. https://doi.org/10.2174/0929867327666200630104550 PMID: 32603272

10. Chu CH, Chen SR, Wu CH, Cheng YC, Cho YM, Chang YK. The effects of negative air ions on cognitive function: An event-related potential (ERP) study. Int J Biometeorol. 2019; 63(10):1309–1317. https://doi.org/10.1007/s00484-019-01745-7 PMID: 31240386

11. Liu RQ, Lian ZW, Lan L, Qian XL, Chen KJ, Hou KS, et al. Effects of negative oxygen ions on sleep quality. Procedia Engineering. 2017; 205:2980–2986.

12. Wiszniewski A, Suchanowski A, Wielgomas B. Effects of air-ions on human circulatory indicators. Polish Journal of Environmental Studies. 2014; 23(2):521–531.

13. Nimmerichter A, Holdhaus J, Mehnen L, Vidotto C, Loidl M, Barker AR. Effects of negative air ions on oxygen uptake kinetics, recovery and performance in exercise: a randomized, double-blinded study. Int J Biometeorol. 2014; 58(7):1503–1512. https://doi.org/10.1007/s00484-013-0754-8 PMID: 24149934

14. Zhao JJ, Zhang L, Xu AG, Zhao YM, Zhao W, Xu QF. Curative effect of low load aerobic exercise in combination with inhalation of air negative oxygen ion on occupational patient with cotton pneumoconiosis. Int J Clin Exp Med. 2016; 9(10):20085–20089.

15. Liu S, Huang QY, Wu Y, Song Y, Dong W, Chu MT, et al. Metabolic linkages between indoor negative air ions, particulate matter and cardiorespiratory function: A randomized, double-blind crossover study among children. Environ Int. 2020; 138:105663. https://doi.org/10.1016/j.envint.2020.105663 PMID: 32203810

16. Jiang S, Ma A, Ramachandran S. Plant-based release system of negative air ions and its application on particulate matter removal. Indoor Air. 2020 Aug 07. https://doi.org/10.1111/ina.12729 PMID: 32767792

17. Dong W, Liu S, Chu M, Zhao B, Yang D, Chen C, et al. Different cardiorespiratory effects of indoor air pollution intervention with ionization air purifier: Findings from a randomized, double-blind crossover study among school children in Beijing. Environmental Pollution. 2019; 254:113054. https://doi.org/10.1016/j.envpol.2019.113054 PMID: 31473392

18. Hyun J, Lee SG, Hwang J. Application of corona discharge-generated air ions for filtration of aerosolized virus and inactivation of filtered virus. Journal of Aerosol Science. 2017; 107:31–40. https://doi.org/10.1016/j.jaerosci.2017.02.004 PMID: 32226115

19. Zhang CY, Wu ZN, Li ZH, Li H, Lin JM. Inhibition effect of negative air ions on adsorption between volatile organic compounds and environmental particulate matter. Langmuir. 2020; 36(18):5078–5083. https://doi.org/10.1021/acs.langmuir.0c00109 PMID: 32279506

20. Goel N, Terman M, Terman JS, Macchi MM, Stewart JW. Controlled trial of bright light and negative air ions for chronic depression. Psychol Med. 2005; 35(7):945–955. https://doi.org/10.1017/s0033291705005027 PMID: 16045061

21. Suzuki S, Yanagita S, Amemiya S, Kato Y, Kubota N, Ryushi T, et al. Effects of negative air ions on activity of neural substrates involved in autonomic regulation in rats. Int J Biometeorol. 2008; 52(6):481–489. https://doi.org/10.1007/s00484-007-0143-2 PMID: 18188611

22. Sirota TV, Safronova VG, Amelina AG, Maltseva VN, Avkhacheeva NV, Sofin AD, et al. Effect of negative air ions on respiratory organs and blood. Biofizika. 2008; 53(5):886–893. PMID: 18954020

23. He P, Chang SL, Zhang YT, Li X, Xie J. Spatial and temporal distribution characteristics of air negative ion concentration in forest recreation areas of xinjiang and its influencing factors. Resources Science. 2015; 37(3):629–635.

24. Wang H, Wang B, Niu X, Song Q, Li M, Luo Y, et al. Study on the change of negative air ion concentration and its influencing factors at different spatio-temporal scales. Global Ecology and Conservation. 2020; 23:e01008.

25. Wu JY, Cheng ZH, Long YZ, Tong FP, Song QA, Liu YG. The variation of aero-anion concentration on landscape forest. Journal of Nanjing Forestry University (Natural Sciences Edition). 2003; 27(4):78–80.

26. Shao HR, He QT, Yan HP, Hou Z, Li T. Spatio-temporal changes of negative air ion concentrations in Beijing. Journal of Beijing Forestry University. 2005; 27(3):35–39.

27. Li AB, Zhao XW, Li CY, Zhou BZ, Yang ZY, Zhou PP, et al. Relationship of plant abundance, air temperature and humidity with negative ions based on control experiment. Chinese Journal of Applied Ecology. 2019; 30(7):2211–2217. https://doi.org/10.13287/j.1001-9332.201907.016 PMID: 31418223

28. Wu RY, Zheng J, Sun YF, Wang QS, Deng CY, Ye D. Research on generation of negative air ions by plants and stomatal characteristics under pulsed electrical field stimulation. Int J Agric Biol. 2017; 19(5):1235–1245.

29. Zhu M, Zhang J, You QL, Banuelos GS, Yu ZL, Li M, et al. Bio-generation of negative air ions by grass upon electrical stimulation applied to lawn. Fresenius Environmental Bulletin. 2016; 25(6):2071–2078.

30. Wu CF, Lai CH, Chu H, Lin WH. Evaluating and mapping of spatial air ion quality patterns in a residential garden using a geostatistic method. Int J Environ Res Public Health. 2011; 8(6):2304–2319. https://doi.org/10.3390/ijerph8062304 PMID: 21776231

31. Yan XJ, Wang HR, Hou ZY, Wang SY, Zhang DY, Xu Q, et al. Spatial analysis of the ecological effects of negative air ions in urban vegetated areas: A case study in Maiji, China. Urban Forestry & Urban Greening. 2015; 14(3):636–645.

32. Hu HQ, Luo BZ, Wei SJ, Wei SW, Wen ZM, Luo SS, et al. Estimating biological carbon storage of five typical forest types in Daxing'anling Mountains, Heilongjiang, China. Acta Ecologica Sinica. 2015; 35 (17):5745–5760.

33. Zhu CY, Ji P, Li SH. Effects of urban green belts on the air temperature, humidity and air quality. Journal of Environmental Engineering and Landscape Management. 2017; 25(1):39–55.

34. Yang J, Luo X, Jin C, Xiao XM, Xia JH. Spatiotemporal patterns of vegetation phenology along the urban–rural gradient in Coastal Dalian, China. Urban Forestry & Urban Greening. 2020; 54:126784.

35. Zhang PY, Li YY, Jing WL, Yang D, Zhang Y, Liu Y, et al. Comprehensive assessment of the effect of urban built-up land expansion and climate change on net primary productivity. Complexity. 2020; 2020:1–12.

36. You W, Zang Z, Zhang L, Li Y, Pan X, Wang W. National-Scale estimates of ground-level PM2.5 concentration in China using geographically weighted regression based on 3 km resolution MODIS AOD. Remote Sensing. 2016; 8(3):184.

37. Li T, Shen H, Yuan Q, Zhang X, Zhang L. Estimating ground-level PM2.5 by fusing satellite and station observations: A geo-intelligent deep learning approach. Geophys Res Lett. 2017; 44(23):11985–11993.

38. Jovanić BR, Jovanić SB. The effect of high concentration of negative ions in the air on the chlorophyll content in plant leaves. Water Air Soil Pollut. 2001; 129(1/4):259–265.

39. Jayaratne ER, J-Fatokun FO, Morawska L. Air ion concentrations under overhead high-voltage transmission lines. Atmos Environ. 2008; 42(8):1846–1856.

40. Krueger AP. The biological effects of air ions. Int J Biometeorol. 1985; 29(3):205–206. https://doi.org/ 10.1007/BF02189651 PMID: 4055123

41. Wu C, Lee GWM. Oxidation of volatile organic compounds by negative air ions. Atmos Environ. 2004; 38(37):6287–6295.

42. Ling X, Jayaratne R, Morawska L. Air ion concentrations in various urban outdoor environments. Atmos Environ. 2010; 44(18):2186–2193.

43. He P, Chang SL, Zhang YT, Li X, Xie J. Spatiotemporal distribution and influence factors of negative air ion in forest recreation areas across Xinjiang. Resources Science. 2015; 37(3):629–635.

44. Chen XL. Investigate the change of negative air ions concentration in Dalian region. Chinese Journal of Physical Therapy. 1986; 3:170–173.

45. Mao HQ, Zhu HJ, Wang XJ, Yang HL, Chen Y. A survey and analysis of the state of air ions in Xining. Journal of Qinghai Medical College. 1994; 15(2):21–26.

46. Wu CC, Zheng QM, Zhong LS. A study of the aero-anion concentration in forest recreation area. Scientia Silvae Sinicae. 2001; 37(5):75–81.

47. Ji YK, Zhou YB, Mi SH, Zhang YN, Ge WZ. Study on air anion concentration in Qipanshan scenic area. Journal of Liaoning Forestry Science & Technology. 2007; 3:16–21.

48. Zhu LN, Wen GS, Wang HX, Xu C. A review on negative air ions. Chinese Agricultural Science Bulletin. 2019; 35(18):44–49.

49. Wang YF, Ni ZB, Wu D, Chen Fan, Lu JQ, Xia BC. Factors influencing the concentration of negative air ions during the year in forests and urban green spaces of the Dapeng Peninsula in Shenzhen, China. Journal of Forestry Research. 2019 Oct 08. https://doi.org/10.1007/s11676-019-01047-z

50. Mao GX, Cao YB, Wang BZ, Wang SY, Chen ZM, Wang JR, et al. The salutary influence of forest bathing on elderly patients with chronic heart failure. Int J Environ Res Public Health. 2017; 14(4):368. https://doi.org/10.3390/ijerph14040368 PMID: 28362327

51. Xie P, Yang J, Wang Hy, Liu Yf, Liu Yl. A new method of simulating urban ventilation corridors using circuit theory. Sustainable Cities and Society. 2020; 59:102162.

52. Zhang PY, Yang D, Zhang Y, Li Y, Liu Y, Cen YF, et al. Re-examining the drive forces of China's industrial wastewater pollution based on GWR model at provincial level. Journal of Cleaner Production. 2020; 262:121309.